CrystEngComm

Accepted Manuscript

ROYAL SOCIETY OF CHEMISTRY

www.rsc.org/crystengcomm

Intermolecular Interactions in Crystalline 1-(Adamantane-1-carbonyl)-3-substituted Thioureas with Hirshfeld Surface Analysis†

Aamer Saeed,[a,*] Michael Bolte,[b] Mauricio F. Erben,[c,*] and Hiram Pérez[d,*]

[a] *Department of Chemistry, Quaid-I-Azam University, Islamabad 45320, Pakistan.*

[b] *Institut für Anorganische Chemie, J.W.-Goethe-Universität, Max-von-Laue-Str.7, D-60438 Frankfurt/Main, Germany.*

[c] *CEQUINOR (UNLP, CONICET-CCT La Plata), Departamento de Química, Facultad de Ciencias Exactas, Universidad Nacional de La Plata, C.C. 962 (1900). La Plata, República Argentina.*

[d] *Departamento de Química Inorgánica, Facultad de Química, Universidad de la Habana, Habana 10400, Cuba.*

† Electronic supplementary information (ESI) available: Tables S1 and S2 list selected bond-distances/angles and ring puckering parameters, respectively, for compound **1**. Revevant data from the Hirshfeld analysis (including C_{XY}, Sx (%), R_{XY} and E_{XY} values) of the main intermolecular interactions for compounds **1-6** are given in Table S3.

Keywords: thiourea, crystal structure, vibrational analysis, hydrogen bonding, Hirshfeld surface analysis.

*Corresponding authors:
(AS) E-mail: aamersaeed@yahoo.com, Tel: +92-51-9064-2128; Fax: +92-51-9064-2241.
(MFE) E-mail: erben@quimica.unlp.edu.ar, Tel/Fax: +54-211-425-9485.
(HP) E-mail: hperez@quimica.uh.cu, Tel: 53-78703922; Fax: 53-78783641.

Abstract

The conformational congested species 1-(adamantane-1-carbonyl)-3-(2,4,6-trimethylphenyl)thiourea has been prepared, fully characterized by elemental analyses, FTIR, ^{1}H, ^{13}C NMR and mass spectroscopy, and the crystal structure determined by using single crystal X-ray diffraction study. The dihedral angle between the plane of 2,4,6-tri-methylphenyl group and the plane of thiourea fragment was optimized by theoretical calculations applying the B3LYP/6-31++G(d,p) level, for the purpose to investigate conformational effects on the stabilization of crystal packing. A detailed analysis of the intermolecular interactions in a series of six closely related phenylthiourea species bearing the 1-(adamantane-1-carbonyl) group have been performed based on the Hirshfeld surfaces and their associated two-dimensional fingerprint plots. The relative contributions of the main intercontacts, as well as the enrichment ratios derived from the Hirshfeld surface analysis establishes the 1-acyl thiourea synton to be a widespread contributor.

1-Introduction

1-Acyl substitued thiourea species have been known since a long time, the preparation of $CH_3C(O)NHC(S)NH_2$ was reported by Neucki as early as 1873.[1] The current and continuously increasing interest in these compounds is probably twofold: 1) potential applications in a wide range of fields are being investigated, and 2) and these compounds are relatively easily prepared. Most promising applications include the use of 1-acyl thioureas as collectors in froth flotation processes,[2, 3] as ionophores in ion selective electrodes,[4-6] and as precursor for metal sulfide nanoparticles.[7, 8] 1-Acyl substitued thiourea species are versatile reagents for the synthesis of a variety of heterocyclic and organosulfur compounds.[9] Furthermore, biological importance of this kind of compounds has been highlighted recently.[10, 11] In particular, substituted 1-(benzoyl)-3-(phenyl) thioureas have been evaluated for antitumor activity with promising results.[12]

As has been recognized, the structural and conformational properties of 1-acyl theories are linked to the achievement of many of these applications. In particular, the formation of proper hydrogen bonds with particular receptors is a key factor acting in many fields, from analytical applications of 1-acyl thioureas as chemosensors for selective and sensitive naked-eye recognition for anions [13-16] as well as in chemical biology and drug design.[17-20]

Increasing attention has been paid to the study of non-covalent interactions acting on the crystal structure and packing of sulfur-containing compounds,[21] a topic of interest not only in organic chemistry,[22] but also in transition metal complexes.[23] Very recently, Eccles at al. [24, 25] demonstrate the versatility of the thioamide functional group [–C(S)NH_2] as a key moiety for crystal engineering. The supramolecular arrangement of 1,2,4-triazole-5-(4H)-thione derivatives involves the formation of a short centrosymmetric $R_2^2(8)$ N–H···S synthon in the solid.[26, 27] It has been shown that the formation of centrosymmetric N–H···S=C hydrogen bond dimer in thiosemicarbazone is favored by the high polarizabilitity of the electron density of the lone pair formally located at the sulfur atom.[28]

The crystal packing of 1-(acyl)-thiourea compounds, with the possibility of different donor and acceptor groups, is usually dominated by hydrogen bonds, mostly determined by both N–H···O=C and N–H···S=C interactions.[29, 30] Bifurcated hydrogen bonds are usually observed,[31-33] the N–H group forming both an intramolecular and intermolecular N–H···O hydrogen bonds.[34] As reported recently,[35] 440 crystal structures for acyl thiourea were searched in the Cambridge Structural Database, the majority (236 structures) displaying a characteristic intermolecular pattern forming dimers *via* N–H···S hydrogen bonding adopting an $R_2^2(8)$ hydrogen-bonding motif.[36] In combination with other patterns, very versatile structures are attainable, including infinite chains,[37] 2-dimensional sheets [38] or 3-dimensional networks.[39] By using periodic system electron density, topological and NBO analysis, we recently showed that strong hyperconjugative lpS→ σ*(N–H) remote interactions -between the molecules forming the dimeric arrange- are responsible for

intermolecular interactions in the simple 1-(2-chlorobenzoyl)thiourea species.[40]

In this article, as part of our ongoing project[41, 42] aimed at understanding the structural features of 1-(adamantane-1-carbonyl)-3-substituted thioureas (see Scheme 1), a novel derivative - namely 1-(adamantane-1-carbonyl)-3-(2,4,6-trimethylphenyl)thiourea– has been synthesized and characterized by single-crystal X-ray diffraction, infrared and nuclear magnetic resonance (NMR) spectroscopies and mass spectrometry. The influence of steric impediment induced by the 2-6-di-methyl substitution in the conformational properties was analyzed by quantum chemical calculations at the B3LYP/6-311++G(d,p). The study of X-ray crystal structure of six adamantane-based acylthiouras reveals that hydrogen bonding and other weaker forces such as π···π and C-H···π interactions participate in a cooperative way to control the supramolecular architectures. Although the π interactions have been widely investigated during the past two decades,[43] an increased number of theoretical and experimental studies have been recently carried out to understand the true nature of π···π and C-H···π interactions.[44-46] These non-covalent interactions could be used as tools in crystal engineering for the design of crystalline adamantane-based thioureas. To get a better understanding of the intermolecular interactions toward the crystal packing, the Hirshfeld surface analysis[47-49] for a series of six closely related 1-(adamantane-1-carbonyl)-3-substituted-phenyl thioureas has been analyzed. Thus, the surfaces of all compounds are mapped by using of d_{norm}, whereas shape-index and curvedness are properties mapped on the surfaces in order to facilitate a more detailed identification of the π-π interactions experienced by molecules in various studied compounds.[44] The present study allowed us to investigate the effect of molecular conformation adopted by the substituted-phenylthiourea group on the stabilization of crystal packing in these compounds, as well as to quantify the propensity of the intermolecular interactions to form the supramolecular assembly.

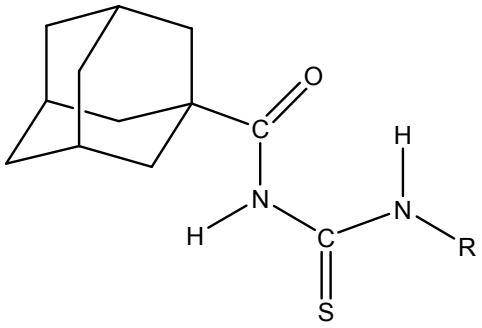

Scheme 1. Representation of 1-(adamantane-1-carbonyl)-3-substituted thioureas.

2-Experimental

2.1-Instrumentation. Melting points were recorded using a digital Gallenkamp (SANYO) model MPD.BM 3.5 apparatus and are uncorrected. ^{1}H and ^{13}C NMR spectra were determined in $CDCl_3$ at 300 MHz and 75.4 MHz respectively using a Bruker spectrophotometer. Fourier transform infrared spectroscopy (FTIR), spectra were recorded on an FTS 3000 MX spectrophotometer (Pakistan). Infrared spectra were recorded in KBr pellets with a resolution of 2 cm^{-1} in the 4000-400 cm^{-1} range on a Bruker EQUINOX 55 FTIR spectrometer (Argentina). Mass Spectra (EI, 70eV) on a GC-MS instrument Agilent technologies, and elemental analyses were conducted using a LECO-183 CHNS analyzer.

2.2- Synthesis of 1-(adamantane-1-carbonyl-3-(2,4,6-trimethylphenyl))thiourea. The reaction sequence leading to the formation of thioureas is depicted in Scheme 2. The starting material 1-adamantane carbonyl chloride was obtained via the reaction of 1-adamantane carboxylic acid with thionyl chloride at room temperature according to the standard procedure [1]. A solution of adamantane-1-carbonyl chloride (10 mmol) in dry acetone (50 ml) was treated with an equimolar quantity of ammonium thiocyanate (10 mmol) in dry acetone (30 ml) and the reaction mixture was refluxed for 30 minutes under nitrogen to afford the adamantane-1-isothiocyanate as intermediate. An equimolar quantity of 2,4,6-trimethylaniline (10 mmol) in acetone (10 ml) was added and the reaction

mixture refluxed for 4 h. On completion (TLC control), the reaction mixture was poured into cold water and the precipitated thiourea (**1**) was recrystallized from aqueous ethanol.

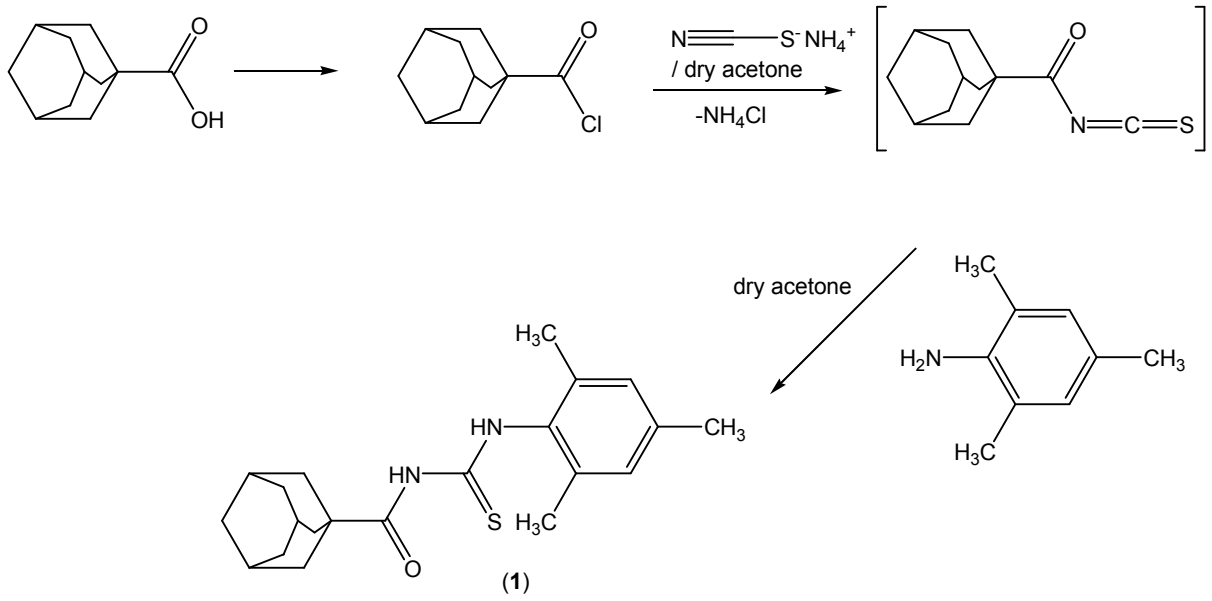

Scheme 2. Synthetic route to 1-(adamantane-1-carbonyl)-3-(2,4,6-trimethylphenyl)thiourea.

1-(Adamantane-1-carbonyl-3-(2,4,6-trimethylphenyl))thiourea (1); yield 87%, mp 196°C. FT-IR (ν cm^{-1}): 3336, 3034, 2909, 2849, 1675, 1575, 1457, 1370; ^{1}H NMR (300 MHz, $CDCl_3$): δ 12.81 (br s, 1H, NH, D_2O exchangeable); 8.73 (br s, 1H, NH, D_2O exchangeable); 7.63 (d, 2H, Ar), 2.31 (s, 3H, $ArCH_3$), 2.11 (s, 6H, $ArCH_3$ x2) 2.12 (brs, 3H, adamantane-CH), 2.03 (s, 6H, adamantane-CH_2), 1.81 (q, 6H, adamantane-CH_2, J = 8.6 Hz); ^{13}C NMR (75.5 MHz, $CDCl_3$): 179.1 (C=S), 176.9 (C=O), 134.1 (Ar), 128.6, 126.9 125.3, 123.6, 121.6 (ArCs), 41.9, 41.9, 39.2, 38.6, 36.1, 36.0, 31.6, 28.0, 27.8 (adamantane-C), 22.3 ($ArCH_3$), 18.7 ($ArCH_3$); Anal. Calcd. for $C_{21}H_{28}N_2OS$ (356.53): C, 70.75; H, 7.92; N, 7.86; S, 8.99 %; Found: C, 71.21; H, 7.89; N, 7.90; S, 8.94%. EIMS m/z: 356.1 (M^+, 41 %).

2.3-Quantum chemical calculations. Optimization geometry was accomplished within the frame work of the density functional theory[50, 51] using the hybrid functional with non-local exchange due

to Becke[52] and the correlation functional due to Lee, Yand and Parr,[53] (B3LYP)as implemented in the Gaussian 03 package.[54] Contracted gaussian basis sets of triple-zeta quality plus polarized and diffuse functions 6-311++G(d,p) for all atoms were used throughout the present work.[55] The corresponding vibrational analyses were performed for the optimized geometries to verify whether they are local minima or saddle points on the potential energy surface of the molecule. Calculated normal modes were also used as an aid in the assignment of experimental frequencies.

2.4-X-ray data collection and structure refinement. The crystal and refinement data for compound **1** are listed in Table 1. Data of compound (**1**) were collected at 173(2) K on a STOE IPDS II two-circle-diffractometer using MoKα radiation. The structure was solved by direct methods [56] and refined with full-matrix least-squares techniques on F^2. All non-hydrogen atoms were refined anisotropically, and all H atoms bonded to C were placed in their calculated positions and then refined using the riding model. The H atoms bonded to N were freely refined. The geometry of the molecule was calculated using the WinGX [57] and PARST [58, 59] software. XP in SHELXTL-Plus [56], ORTEP-3 [60] and Mercury [61] programs were used for molecular graphics.

Full crystallographic data for compound **1** have been deposited with the Cambridge Crystallographic Data Centre (CCDC 1410273). Enquiries for data can be directed to: Cambridge Crystallographic Data Centre, 12 Union Road, Cambridge, UK, CB2 1EZ or (e-mail) deposit@ccdc.cam.ac.uk or (fax) +44 (0) 1223 336033.

Table 1. Crystal data and structure refinement for compound **(1)**.

Empirical formula	$C_{21}H_{28}N_2OS$
Formula weight	356.51
Temperature / K	173(2)
Crystal system	triclinic
Space group	P-1
Unit cell dimensions	a =7.6584(7) Å
	b =10.2121(8) Å
	c =13.1295(11) Å
	α =108.228(6)^o
	β= 97.789(7)^o
	γ= 92.502(7)^o
Volume / Å^3	962.26(15)
Z	2

ρ calc. / mg mm^{-3}	1.230
μ / mm^{-1}	0.179
F(000)	384
Crystal size / mm^3	0.35 x 0.29 x 0.27
Theta range for data collection	3.30 to 27.62°
Index ranges	-9<=h<=9, -12<=k<=13, -17<=l<=17
Reflections collected	18032
Independent reflections	4399 [R(int) = 0.061]
Data/restraints/parameters	4399/0/238
Goodness-of-fit on F^2	1.054
Final R indexes [I >2σ (I)]	$R1$ = 0.0409, $wR2$ = 0.1064
Final R indexes [all data]	$R1$ = 0.0434, $wR2$ = 0.1084
Largest diff. peak/hole / e Å^{-3}	0.316 / -0.290

2.5-Hirshfeld surface computational method. Hirshfeld surfaces and their associated two-dimensional fingerprint plots[62-65] are generated using CrystalExplorer3.1 software.[66] The d_{norm} (normalized contact distance) surface and the breakdown of two-dimensional fingerprint plots are used for decoding and quantifying intermolecular interactions in the crystal lattice.[67-69] The d_{norm} is a symmetric function of distances to the surface from nuclei inside and outside the Hirshfeld surface (di and de, respectively), relative to their respective van der Waals radii. A color scale of red (shorter than vdW separation)—white (equal to vdW separation)—blue (longer than vdW separation) is used to visualize the intermolecular contacts. The 3D d_{norm} surfaces are mapped over a fixed color scale of -0.24 (red) to 0.93 Å (blue), *shape-index* mapped in the color range of -1.0 au (concave) –1.0 au (convex) Å, and *curvedness* in the range of -4.0 au (flat) – 0.01 au (singular) Å. The 2D fingerprint plots are displayed by using the translated 0.6–2.6 Å range, and including reciprocal contacts.

3-Results and Discussion

3.1- Conformational properties

Previous structural studies on 1-(adamantane-1-carbonyl)-3-mono substituted thioureas have shown that a local planar structure of the acyl-thiourea group is preferred, with opposite orientation between the C=O and C=S double bonds ("*S*-shape").[41, 42, 70] In the present case, a similar

conformational behaviour has been computationally determined for 1-(adamantane-1-carbonyl)-3-(2,4,6-tri-methylphenyl)thiourea, with the 1-acyl thiourea group adopting the *S*-shape and the substituted phenyl ring nearly perpendicular to the mean plane defined by the 1-acyl thiourea group. It is worthy to notice that the molecule isolated in vacuum displays nearly-perfect C_S symmetry.

For comparison purposes, similar calculations have been done for the related 1-(adamantane-1-carbonyl)-3-(phenyl)thiourea. For this species, the most stable form displays the same *S*-shape conformation, but on the contrary, the phenyl ring coplanar with the 1-acyl thiourea group. Thus, it becomes apparent that the conformation adopted by the 2,4,6-tri-methyl group is determined by strong steric impedance caused by the interaction between the C=S bond with the methyl groups occupying the 2,6-positions. The computed molecular structure is in very good agreement with the experimental one (see Section 3.3).

3.2- Vibrational properties

The determination of the vibrational properties of 1-acyl thioureas has showed to be a powerful tool for analyzing conformational and structural features in the solid state.[36] The FTIR spectrum of **(1)** have been measured and compared with the calculated [B3LYP/6-311++G(d,p)] harmonic frequencies. The experimental and simulated spectra are shown in Figure 1. Two well-defined absorptions are observed in the infrared spectrum at 3426 and 3231 cm^{-1}, the last one with higher intensity, which can be associated with the ν(N–H) stretching modes.[71] This spectral region is well reproduced by quantum chemical calculations with the corresponding harmonic frequencies computed at 3613 (56.6) and 3393 (366.5) cm^{-1} (computed intensities, in Km/mol, are given). The formation of the intramolecular N1–H···O1=C hydrogen bond is responsible for the impressive red-shift and a strong intensification of the ν(N1–H) normal mode as compared with the second ν(N2–H) stretching, in agreement with previous data for related species.[72] This interaction also affect the

force constant of the ν(C=O) stretching mode,[73] which is observed as an intense and symmetric band at 1674 cm^{-1} in the infrared spectrum in good agreement with the computed value (1707 cm^{-1}).

The most intense absorption is observed as a rather broad band at 1511 cm^{-1} in the infrared spectrum, which can be assigned to the δ(N–H) deformation modes, in agreement with previous reported values for 1-acyl-3-mono-substituted thioureas.[74, 75] The computed spectrum shows two intense absorptions at similar frequencies values [1567 (350.9 Km/mol) and 1546 (628.6 Km/mol) cm^{-1}] that are associated with the δ(N1–H) and δ(N2–H) normal modes, respectively.

The medium intensity absorptions observed at 772 and 751 cm^{-1} are assigned to the characteristic "breathing mode" of the adamantane group [76] and to the ν(C=S) stretching mode, respectively. The last assignment is in agreement with previously studied thiourea derivatives [75, 77] and suggest that the C=S group is acting as a H bond-acceptor . It is well-known that the formation of C=S···H–X intermolecular hydrogen bonds effect the frequency of the ν(C=S) mode.[78]

Thus, based on the analysis of the main features of the infrared spectra it is concluded that compound **(1)** forms strong intra- and inter-molecular interactions in the solid, most probably due to the formation of hydrogen bonds involving the N1–H group as a donor and carbonyl and thiocarbonyl groups as acceptors.

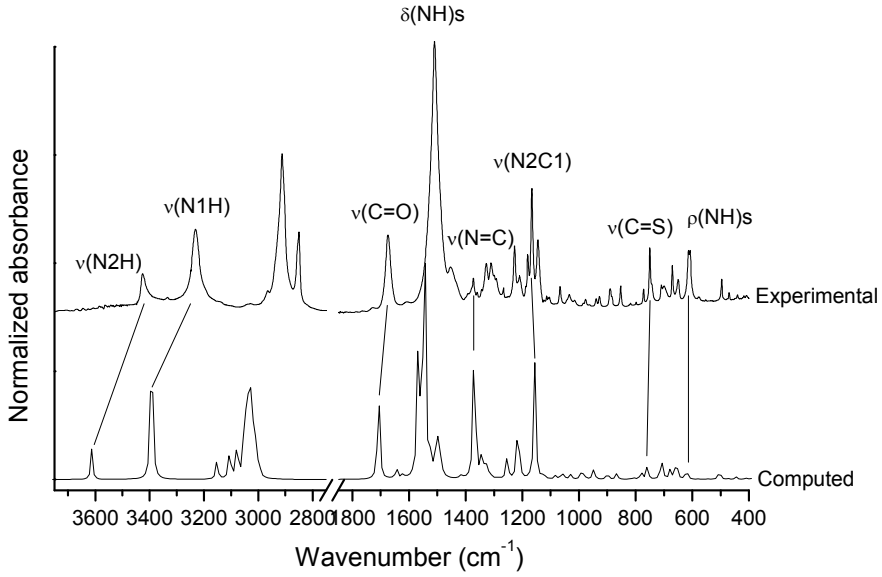

Figure 1. Computed [B3LYP/6-311++G(d,p)] and experimental (FTIR) infrared spectra of **1**.

3.3-Crystal Structure Determination

The X-ray geometrical parameters around the central 1-acyl thiourea moiety of compound **1**, together with the computed [B3LYP/6-311++G(d,p)] values are listed in Table S1 in the electronic supplementary information (ESI). The ORTEP view of the X-ray structure -with atomic labeling- is shown in Figure 2, together with the computed molecular structure. The geometric parameters of hydrogen bonds for compound **1** are shown in Table 2. An intramolecular N–H···O hydrogen bond (H···O = 2.08(2) Å, N···O = 2.723(2) Å, ∠N–H···O = 134°) is present, forming a six-membered ring commonly observed in this type of compounds,[79] which confirms the results of the vibrational data. The central -C(O)-NH-C(S)-NH- fragment is planar, with the C=O and C=S bonds in opposite orientation, adopting a ‘‘*S*-shape’’ in agreement with close structures of 1-acyl-3-mono-substitued thioureas.[32] The observed C=S and C=O double bonds, as well as the shortened C–N bond lengths (Table S1), are typical of thiourea compounds.[80] The dihedral angle between the best planes through the thiourea moiety CNC(S)N and the 2,4,6-tri-methyl group is 89.56(5)°, in agreement with the

theoretical calculations (see section 3.1). This value is also similar for related structures with the same nature of substituents on the 2,4,6-tri-substituted group.[81] The ring puckering parameters [82] for the cyclohexane rings of the adamantane group are given in Table S2 in the electronic supplementary information (ESI). The q(3) puckering amplitude values are very longer than the corresponding q(2) amplitude values, which are very close to zero. The q(3) values are also very similar to the total puckering amplitudes QT with average value of 0.625 Å, which lies only slightly under the QT value of 0.63 Å for ideal cyclohexane chair.[82] These results indicate that all cyclohexane rings in the adamantane group adopt a very slightly distorted chair conformation.

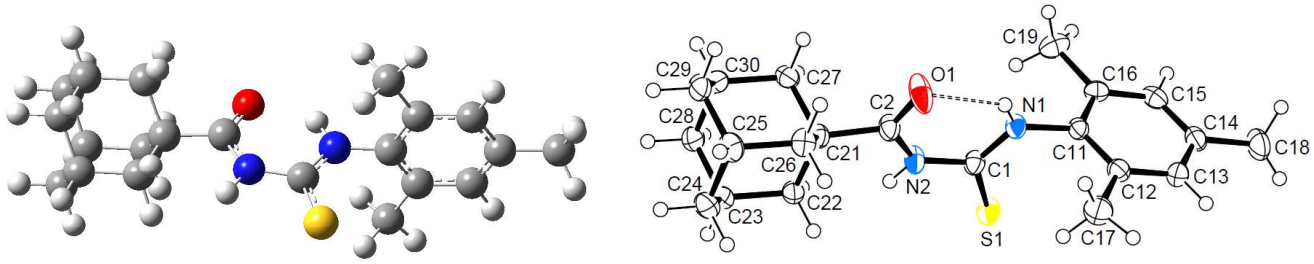

Figure 2. Computed (left) and X-ray (right) molecular structure of **1** with displacement ellipsoids plotted at 50% probability level. Intramolecular N–H···O hydrogen bond is shown as dashed lines.

In the crystal packing of **1**, intermolecular N–H·· O and non-conventional C–H···S hydrogen bonds link the molecules into centrosymmetric dimers stacked along the direction of the *b* axis (Figure 3), giving $R_2^2(12)$ and $R_2^2(14)$ graph-set motifs, respectively.

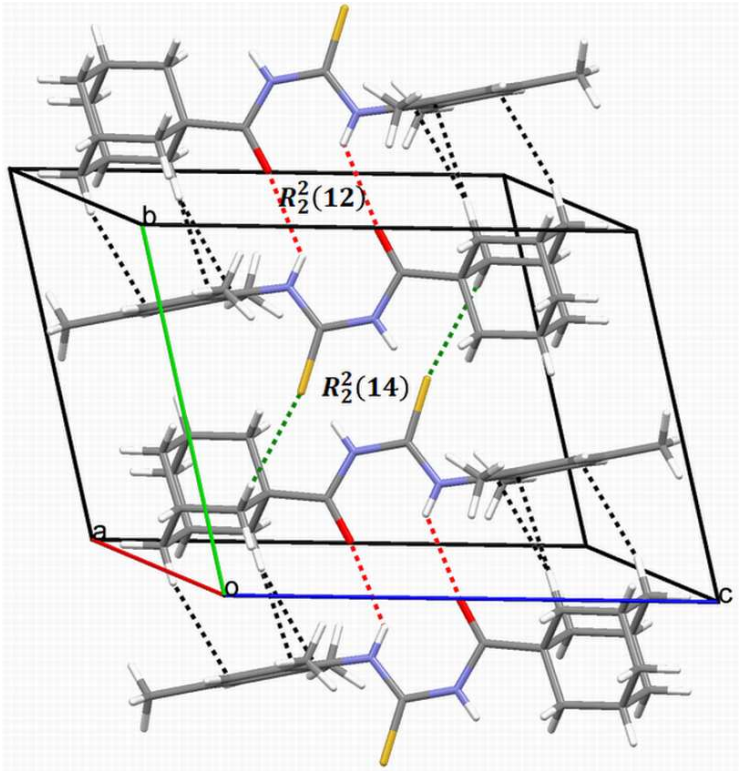

Figure 3. A packing diagram of compound **1** showing centrosymmetric dimers stacked along *b*-axis. Intra- and intermolecular hydrogen bonds are shown as dashed lines.

Table 2. Hydrogen bonding geometry for compounds **1-6** (Å, °).

Compound	*D*—H···*A*	*d*(*D*—H)	*d*(H···*A*)	*d*(*D*···*A*)	∠(*D*—H···*A*)	Label (Fig. 3)
1	N1—H1···O1^{i}	0.83(2)	2.40(2)	3.041(2)	132	1
	C27—H27B···S1^{ii}	0.99	2.986(1)	3.916(1)	157	6
2						
	N102—H102···S2^{i}	0.83	2.77(2)	3.576(2)	162	1
	C110—H11B···S2^{i}	0.99	2.7031(5)	3.652(2)	161	2
	S1···H21J^{i}	-	2.7110(5)^{a}	-	-	3
	S1···H202^{i}	-	2.75(2)^{a}	-	-	4
	C105—H10B···O202^{ii}	0.99	2.544(1)	3.412(2)	152	5
	C112—H11E···O203^{iii}	0.99	2.404(1)	3.380(2)	169	9
	C106—H10C···C112^{iv}	0.95	2.843(2)	3.649(2)	143	10
3						
	N2—H2···S1^{i}	0.89	2.66(1)	3.499(1)	157	1
	C14—H14A···S1^{i}	0.99	2.7829(4)	3.710(1)	156	2
	C6—H6A···O2^{ii}	0.95	2.482(2)	3.077(2)	121	3
	C14—H14B···O3^{iii}	0.99	2.646(1)	3.526(2)	148	4
4						
	N2—H2···S1^{i}	0.80	2.84(2)	3.592(1)	155	1
	C22—H22B···S1^{i}	0.99	2.7744(5)	3.704(2)	157	2
	C26—H26A···S1^{i}	0.99	2.9861(4)	3.865(2)	148	3
	C29—H29A···Cl2^{ii}	0.99	2.834(1)	3.715(2)	149	4
	C22—H22A···C16^{iii}	0.99	2.895(2)	3.812(3)	154	5
5						

	N1—H1···O1^{i}	0.88	2.30(3)	3.038(4)	141	1
	C13—H13···F2^{ii}	-	2.380(2)	-	-	2
	C23—H23···F1^{iii}	1.00	2.661(2)	3.624(4)	161	3
	C26—H26A···S1^{iv}	0.99	2.9123(9)	3.830(3)	154	4
	C27—H27A···S1^{iv}	0.99	2.9650(9)	3.867(3)	152	5
6						
	N1—H1···O2^{i}	0.79(3)	2.52(3)	3.184(3)	142	1
	O1—H10···S1^{ii}	0.86(3)	2.36(3)	3.212(2)	169	3
	C14—H14A···S1^{iii}	0.97	2.8411(7)	3.761(2)	159	4
	C3—H3···O1^{iv}	0.93	2.628(2)	3.504(3)	157	5
	C14—H14B···F1^{v}	0.97	2.449(2)	3.354(3)	155	6

Symmetry codes for **(1):** (i) 1-x,-y,1-z; (ii) 1-x,1-y,1-z; for **(2):** (i) x,y,z; (ii) -½+x,½-y,-½+z; (iii) 3-x,1-y,1-z; (iv) 2.5-x,-½+y,½-z; for **(3):** (i) 1-x,1-y,-z; (ii) x,1.5-y,-½+z; (iii) -x,½+y,-½-z; (iv) -x,1-y,-z; for **(4):** (i) 1-x,1-y,2-z; (ii) -1+x,y,1+z; (iii) 1-x,1-y,1-z; (iv) x,1.5-y,-½+z; for **(5):** (i) 1-x,y,½-z; (ii) x,1+y,z; (iii) 1+x,y,z; (iv) 1-x,-y,1-z; for **(6):** (i) 2-x,1-y,1-z; (ii) 1-x,-y,2-z; (iii) 2-x,-y,1-z; (iv) 3-x,-y,2-z; (v) -1+x,y,z; [a]The *A*···H reciprocal interaction.

3.4- Hirshfeld surface analysis

Hirshfeld surface analysis was carried out for the purpose to study the nature of intermolecular contacts and theirs quantitative contributions to the supramolecular assembly of **1**, as well as on other five mono-substituted adamantyl phenylthiourea derivatives recently reported.[41, 42, 83] The selected structures are labelled here as **2**: 1-(adamantane-1-carbonyl)-3-(3-nitrophenyl)thiourea, **3**: 1-(adamantane-1-carbonyl)-3-(4-nitrophenyl)thiourea, **4**: 1-(adamantane-1-carbonyl)-3-(2,4-dichlorophenyl)thiourea, **5**: 1-(adamantane-1-carbonyl)-3-(2-bromo-4,6-difluorophenyl)thiourea, and **6**: 1-(adamantane-1-carbonyl)-3-(2,6-difluoro-4-hydroxyphenyl)thiourea. The geometric parameters of hydrogen bonds for compounds **1-6** are shown in Table 2.

The Hirshfeld surfaces of the compounds **1-6** are shown in Figure 4. The d_{norm} map of compound **1** indicates that H···O reciprocal contacts are distinguished relative to the other interactions by a pair of adjacent deep-red regions, labelled 1, attributed to strong N—H···O hydrogen bonds (Table 2) forming $R_2^2(12)$ dimers as described in Figure 3. The same type of interaction was only observed (labelled 1) for the structures **5** and **6**. A pair of pale blue to white spots for structures **1** (labelled 6), **5** (labelled 4) and **6** (labelled 4) represent H···S contacts that indicate C···H contacts associated to two T-shaped C—H···π interactions as described in Table 3. The distances between the involved H-atoms (H13 and H22A) and the nearest carbon atom in the

corresponding benzene ring are in agreement with theoretical calculatons for related compounds.[84] For structures **2**, **3** and **4** (labelled 1) this motif is combined with N—H···S hydrogen bonds forming typical centrosymmetric $R_2^2(8)$ loops. It is worthwhile to highlight here that the dihedral angles of 65.22(2) and 71.61(3)^o between the plane of central thiourea grouping and the plane of the 2,4,6-trisubstituted phenyl ring for structures **5** and **6**, respectively, are the closest to the one obtained for structure **1**. The corresponding angles for structures **2**, **3** and **4** measure 51.15(1), 37.22(2) and 39.38(1)^o, respectively. The differences in the dihedral angle for structures **5** and **6** related to structure **1** could be attributed to the presence of two types of substituents in the phenyl ring. For compound **1**, the supramolecular arrangement is further controlled by two T-shaped C—H···π interactions involving the H26B and H29B atoms of adamantane group, and C11-C16 bencene ring [centroid Cg(1); symmetry: 1-x,-y,1-z]. The shorter interaction[85] is found with H26B···Cg(1) as described in Table 4. The distance of 2.820(1) Å between H26B atom and the nearest carbon atom in the benzene ring is in agreement with theoretical calculations.[84]

Table 3. Geometrical parameters for the π-stacking moieties involved in the π···π interactions for compounds **2**, **3** and **6** (Å, ^{o})

rings I-J[a]	*R*c[b]	*R*1v[c]	*R*2v[d]	α[e]	β[f]	γ[g]	symmetry
			Compound **2**				
Cg(1)···Cg(2)	3.656(1)	3.291(1)	3.317(1)	2.03	24.9	25.8	1.5-x, -½+y, ½-z
Cg(1)···Cg(2)	3.784(1)	3.371(1)	3.332(1)	2.03	28.3	27.0	2.5-x, -½+y, ½-z
			Compound **3**				
Cg(1)···Cg(2)	4.670(1)	3.324(2)	3.324(2)	0.00	44.6	44.6	-x, 1-y, -z
			Compound **6**				
Cg(1)···Cg(2)	4.101(2)	3.371(2)	3.371(2)	0.00	18.3	18.3	2-x, -y, 2-z

[a] Cg(1) and Cg(2) are the centroids of the rings C102-C107 and C202-C207 for (**2**), respectively, and C1-C6 for (**3**) and (**6**). [b] Centroid distance between ring I and ring J. [c] Vertical distance from ring centroid I to ring J. [d] Vertical distance from ring centroid J to ring I. [e] Dihedral angle between mean planes I and J. [f] Angle between the centroid vector Cg(I)···Cg(J) and the normal to the plane (I). [g] Angle between the centroid vector Cg(I)···Cg(J) and the normal to the plane (J).

Figure 4. Views of the Hirshfeld surfaces in two orientations for compounds **1-6**. Thermal ellipsoids at 50% probability level. Surface in column 3 rotated by 180° around the horizontal axis of the plot; H-atoms are omitted; numbered arrows are described either in Table 2 or in text.

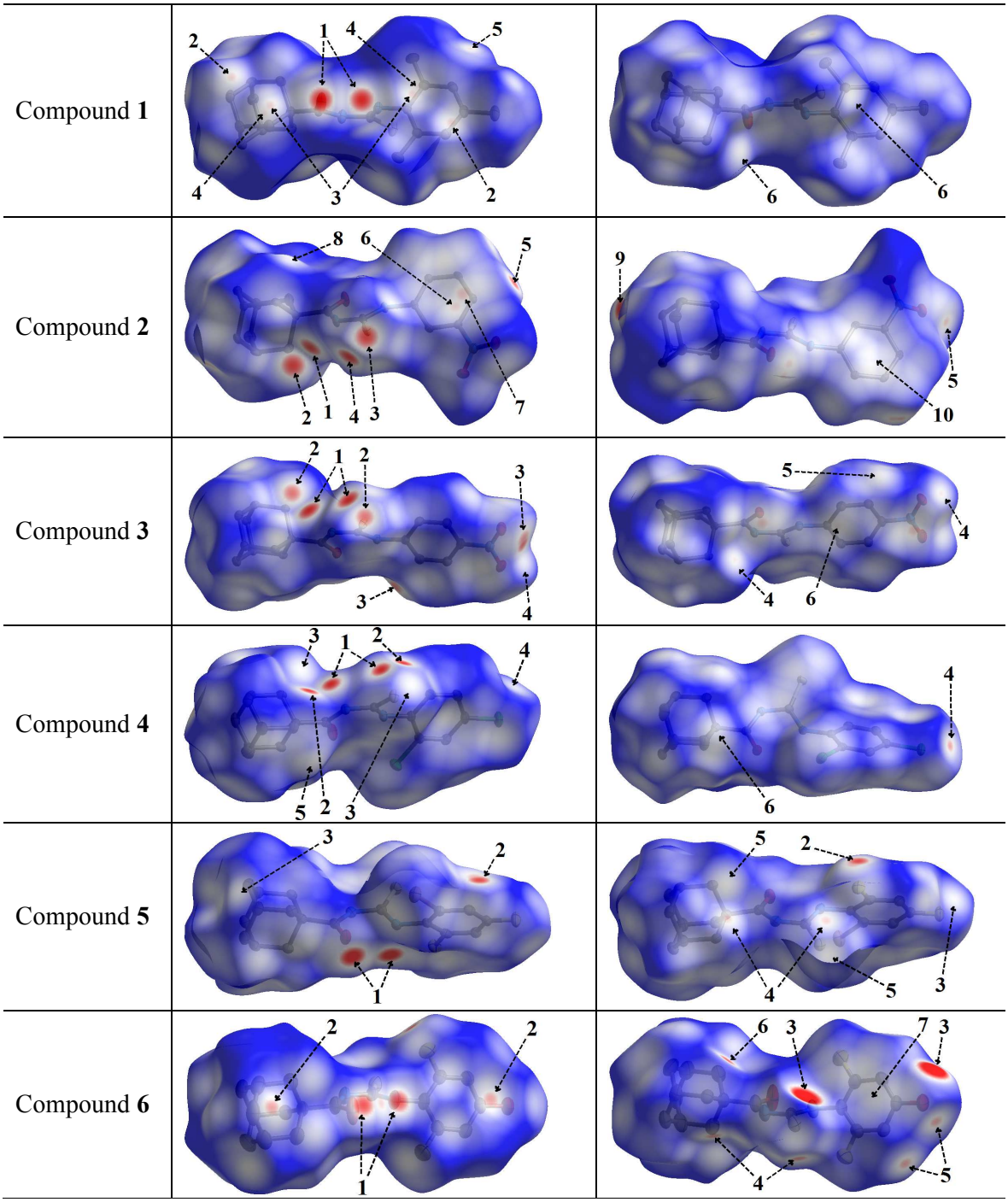

Table 4. Geometrical parameters of C-H···π interactions* for compounds **1** and **4** (Å, °)

C-H•••Cg(J)[a]	H•••Cg1	H-perp[b]	γ[c]	∠C-H•••Cg(J)	H•••C[d]	symmetry
			compound **1**			
C26-H26B···Cg(1)	2.70	2.66	10.7	162	2.820(1)	1-x,-y,1-z
			compound **4**			
(R1)C13-H13···Cg(1)	2.85	2.84	3.50	135	3.090(2)	x,1.5-y,-½+z
(R2)C22-H22A···Cg(1)	2.87	2.80	14.72	127	2.895(2)	1-x,1-y,1-z

[*] (H•••Cg1 < 3.0 Å, γ < 30.0°). [a] Centroid of benzene ring. [b] Perpendicular distance of H to ring plane J. [c] Angle between the Cg-H vector and ring J normal. [d] Distance between H-atom and the nearest carbon atom in the benzene ring. R1 denotes a puckered ring of adamantane group, and R2 of benzene ring.

The N—H···S, C—H···S and C—H···O hydrogen bonds are present in the structures **2** and **3**, and can be seen as deep-red spots labelled 1, 2 and 5, respectively, with similar values for the corresponding H···A distances (Table 2). However, when the nitro group is at *meta* position on the phenyl ring (structure **2**), the d_{norm} map shows H···C contacts (labelled 10) attributed to C—H···C hydrogen bond, involving the hydrogen at position 5 on the phenyl ring. In addition, this hydrogen atom form H···O and H···H contacts which are not visible in the two selected orientations of d_{norm} map. These interactions are responsible for the increase of the dihedral angle between the plane of thiourea fragment and the plane of 3-nitro-phenyl ring in comparison to that for 4-nitro-phenyl conformation in the structure **3** (values are given above).

In the halophenylthioureas **4** and **5**, X—H···S (X = N, C) contacts are manifested as deep-red spots (labelled 1 and 2) for the former, whereas deep-red regions (labelled 1) are attributed to the presence of N—H···O hydrogen bonds for the structure **5**. The H···D (D = Cl, F) contacts are visible as small red spots, labelled 3 and 2, associated to C—H···Cl and C—H···F hydrogen bonds, respectively. Unlike the structure **5**, the d_{norm} map for structure **4** shows a red spot (labelled 5) associated to C—H···C hydrogen bond. It is common for all the six compounds the existence of H···H contacts with red to white regions in the Hirshfeld surfaces. In the case of structure **6** two deep-red regions (labelled 3) correspond to strong O–H···S hydrogen bonds associated with the presence of hydroxyl groups. In the d_{norm} surfaces of **1**, **2**, **3** and **4** there are red to white spots labelled 5, 8, 5 and 6, respectively, due to H···H contacts with distances ranging from 2.325 to 2.391 Å, according to the structural determinations.

The red to white areas marked as 6 and 7 for surface of **2**, and 7 for surface of **6** are C···C contacts representative of π···π stacking interactions (Table 3). The pattern of adjacent red and blue triangles that appears on the *shape index* surfaces of **2** and **6**, as well as a relative large and flat green region at the same side of the molecule on the corresponding *curvedness* surfaces confirm the presence of π···π interactions (Figure 5). The largest region of flat curvedness appears for compound **2**. This type of intermolecular contact is also evident by using of these properties mapped on the surface of **3** as showed in Figure 5, but its geometric parameters given in Table 3, particularly *R*c, β and γ indicate a weaker interaction, in comparison with those on the surfaces **2** and **6**. In addition, a relative smaller region of flat curvedness on the surface of **3** allows us estimate the existence of π···π stacking with a minor overlapping of the adjacent molecules.

Figure 5. Hirshfeld surfaces mapped with *shape-index* and *curvedness* for compounds **2**, **3** and **6**.

Compound **2**	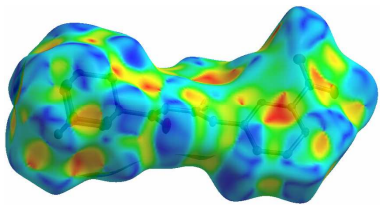	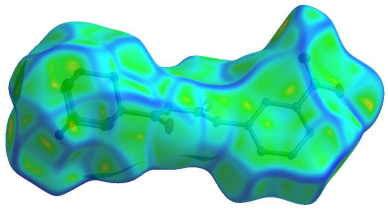
Compound **3**	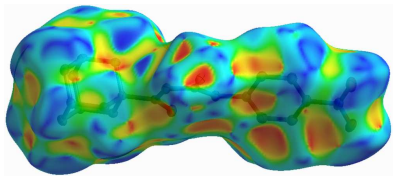	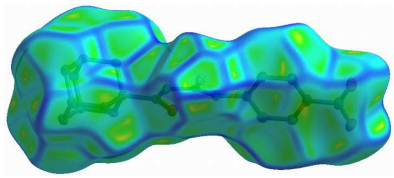
Compound **6**	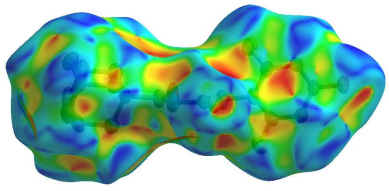	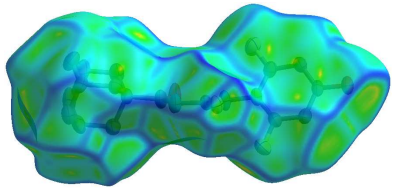

Fingerprint plots for the main intermolecular contacts for all the six structures are shown in Figure 6. For structure **1** the shortest contacts correspond to the very close H···H contacts, showing a sharp spike centred (labelled 1) near a (d_e + d_i) sum of 2.1 Å. The O···H (labelled 2) and C···H

contacts (labelled 3), with sharp pairs of spikes centered near a (d_e + d_i) sum of 2.3 and 2.9Å, correspond to N—H···O and C—H···C hydrogen bonds, respectively. In addition, we observe S···H contacts (labelled 4) with less sharper spikes centered around (d_e + d_i) of 2.8 Å, attributed to C—H···S hydrogen bonding (Table 2). The H···H contacts are shortest for each of the compounds, and O···H, S···H and C···H intermolecular contacts are present in all the structures. In the case of structures **3** and **4**, the distances of C···H and O···H contacts, respectively, are longer than the sum of van der Walls radii. Unlike the compound **1**, there are O···H reciprocal contacts with asymmetric pair of spikes for structure **2**, indicating H···O and O···H contacts with significantly different (d_e + d_i) distances, near of 2.3 and 2.5 Å, respectively. C···C contacts (labelled 5) attributed to π···π interactions between phenyl rings were observed for the structures **2** and **6,** with centroid-to-centroid distances of 3.656(2) and 4.101(3)Å, respectively. The corresponding fingerprint plots clearly depicts a green area on the diagonal at approximately 1.8 Å, which is characteristic of π···π interactions. The pairs of spikes (labelled 6 and 7) in the halophenylthioureas **4** and **5** correspond to Cl···H and F···H contacts, respectively. Fingerprint of structure **5** reveals the occurrence of weak Br···H interactions (labelled 8), which are not visible in the Hirshfeld surfaces due to the distances are longer that sum of van der Waals cutoff radii.

Figure 6. Fingerprint plots for compounds **1-6**. Close contacts are labelled as: (1) H···H, (2) O···H, (3) C···H, (4) S···H, (5) C···C, (6) Cl···H, (7) F···H, (8) Br···H.

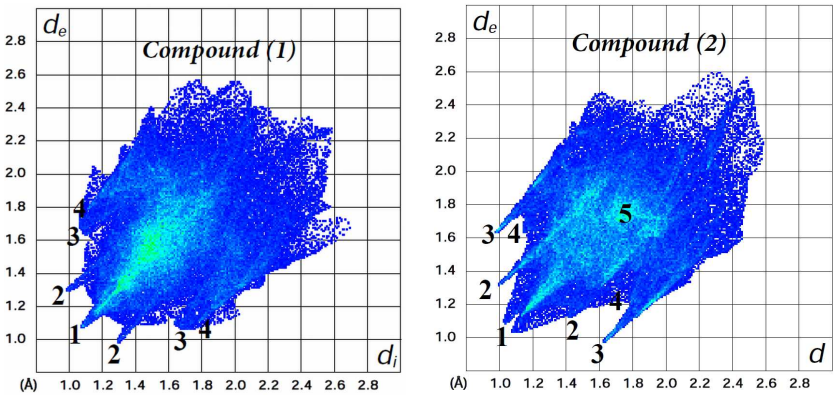

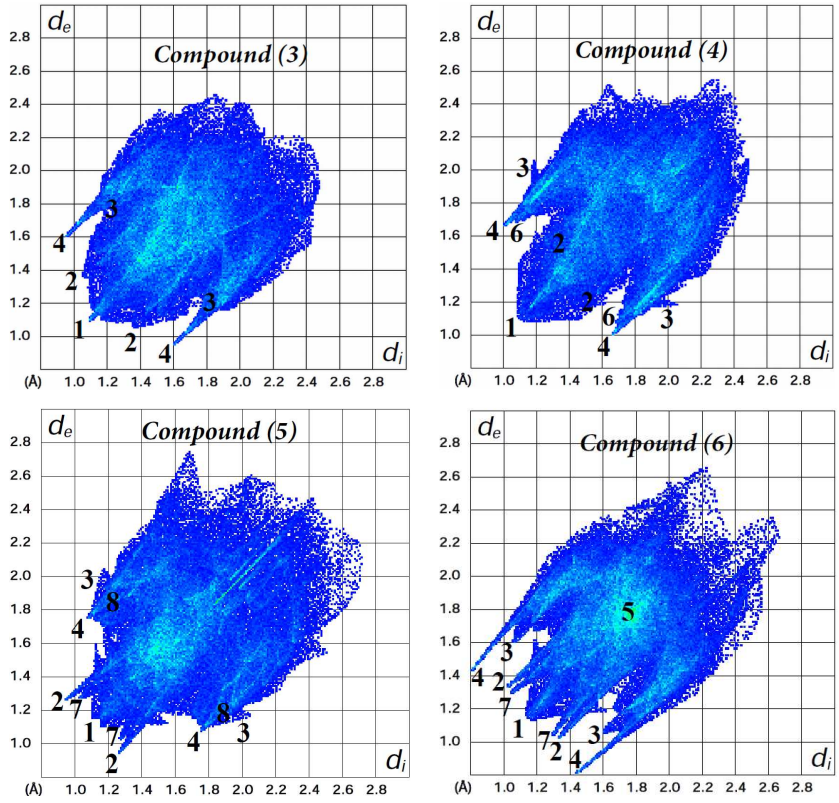

The relative contributions to the Hirshfeld surface area due to main intermolecular contacts for the compounds **1**-**6** are shown as a histogram in Figure 7. It is clear that the nature, number and position of the substituents on the phenyl ring play a key role in the participation of each type of contact. For all the structures the H···H interactions (labelled 1) have the most important contribution to the total Hirshfeld surface. In the structure **1**, the major presence of eleven hydrogen atoms on the phenyl group, notably increases the contribution from H···H over the Hirshfeld surface (72.0 %) regarding the other five structures. However, according to crystal structure determination the lowest percentage of H···H contacts for structure **5** (33.9 %) is a result of interactions involving the adamantane and phenyl groups. For the contacts associated to hydrogen bonds the contributions of S···H contacts are very similar (9.5-12.8 %) due to all the six structures contain only one sulfur atom involved in the formation of dimers through C—H···S hydrogen bonds. The percentages of C···H contacts present less close interval of (8.3-14.2 %). In the case of structures **2** and **3** the O···H interactions show the highest Hirshfeld contact surfaces of 26.4 and 17.9 %, respectively, The N···H

contacts are only visible for compounds **2** and **3**, with the smallest fingerprint contributions of 4.6 and 3.6 %, respectively. Other types of intermolecular contacts with the most important percentages such as C···C (3.4 %) occur for compound **2**, and C···O (3.0 %), N···O (2.2 %) and O···O (2.4 %) for compound **3**.

Figure 7. Relative contributions of intermolecular contacts to the Hirshfeld surface area for compounds **1-6.**

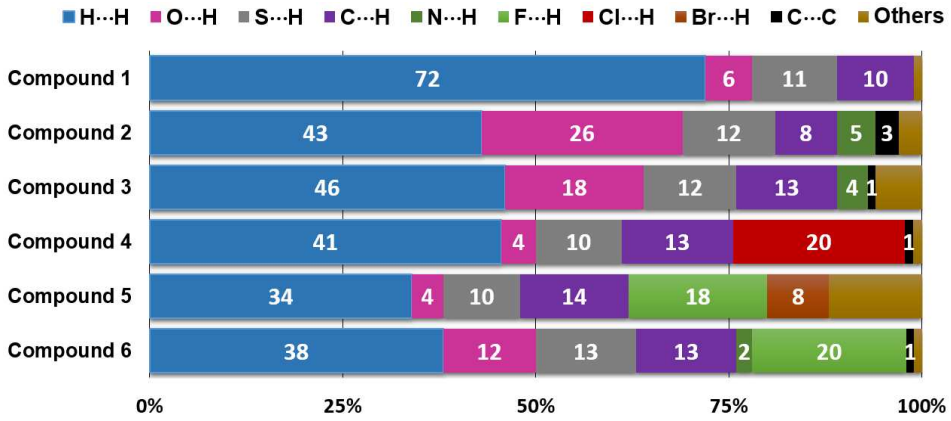

In this study, we have calculated the enrichment ratios[86] of the main intermolecular contacts for compounds **1-6** in order to analyze the propensity of two chemical species (X,Y) to be in contact. The enrichment ratio E_{XY} is a descriptor derived from the Hirshfeld surface analysis, and defined as the ratio between the proportion of actual contacts C_{XY} in the crystal, and the theoretical proportion of random contacts R_{XY}. The percentages of Hirshfeld surface contacts C_{XY} are given by CrystalExplorer3.1.[66] The proportion S_X of different chemical species on the molecular surface is obtained from C_{XX} and C_{XY} values. The random contacts R_{XY} values are calculated from the corresponding S_X and S_Y proportions by using of probability products. The value of E_{XY} is expected to be generally larger than unity for pairs of elements with high propensity to form contacts in crystals, while pairs that tend to avoid contacts are associated with E_{XY} values lower than unity.

Table 5 shows the enrichment ratios of the main intermolecular interactions for compounds **1-6** (the whole information is provided in Table S3). The H···H contacts can be considered as

favoured in all structures due to enrichment ratios are very close to unity (E_{HH} = 0.90-0.98), and constitute most of the interaction surface (33.9-72.0 %). The E_{SH} values are larger than unity (1.12-1.49) for all the structures, indicating that S···H contacts have an increased likelihood to form in the crystal packing, with similar random contacts ranging from 8.1 to 9.4 %. The E_{CH} ratios ranging from 1.10 to 1.37 (except structure **2**) indicate that C···H contacts have a high propensity to form in crystal packing, as result of abundant S_H proportion of hydrogen atoms (61.4-85.6%) at the molecular surfaces. The O···H contacts of all the structures are much enriched (except structure **3**), with the highest propensity for structures **2** and **6**. Despite the contribution of O···H contacts to the Hirshfeld surface (C_{OH} = 11.9 %) for compound **6** is lower than that for structure **3** (C_{OH} = 17.9 %), the proportion of oxygen atoms on the molecular surface of the former is significantly smaller (S_O = 6.5%), decreasing the value of the random contacts (R_{OH} = 8.7%). This allows to explain the higher propensity of the O···H contacts for structure **6** (E_{OH} = 1.37) in comparison with that of the structure **3**.

Table 5. Enrichment ratios E_{XY} of the main intermolecular interactions for compounds **1-6**.

Interaction	**1**	**2**	**3**	**4**	**5**	**6**
H···H	0.98	0.91	0.97	0.98	0.90	0.84
C···H	1.17	0.73	1.10	1.12	1.37	1.20
N···H	0.83	1.21	0.90	0.19	/	1.15
O···H	1.15	1.35	0.93	1.02	1.16	1.37
S···H	1.12	1.44	1.46	1.14	1.19	1.49
F···H	-	-	-	-	1.44	1.35
Cl···H	-	-	-	1.07	-	-
Br···H	-	-	-	-	0.77	-
C···C	-	4.86	0.71	1.00	-	/
C···O	-	0.58	1.30	-	-	-
N···O	-	1.00	2.72	-	-	-
O···O	-	-	1.20	-	-	-

E_{XY} for random contacts R_{XY} lower than 0.7% were not calculated.

The E_{FH} values of 1.44 and 1.35 in the halophenylthioureas **5** and **6**, respectively, as well as the E_{ClH} value of 1.07 for structure **4** reveal that F···H a nd Cl···H contacts are highly favoured, with the highest proportion of S_F (10.3 and 10.8%) and S_{Cl}(14.2%), respectively, apart from the S_H values. This indicates that the weak fluorine and chlorine hydrogen bonding interactions are

comparable in importance to the characteristic strong N—H···O hydrogen bonds [86-88] in acylthiourea derivatives. Other types of contacts that appear in structure **6** involving fluorine atoms, such as C···F, N···F and O···F contacts are very impoverished. The N···H contacts are highly favoured for structures **2** and **6** (E_{NH} = 1.21 and 1.15), slightly favoured for structures **1** (E_{NH} = 0.83) and **3** (E_{NH} = 0.90), and impoverished for compounds **4** and **5**, with E_{NH} ratios of 0.19 and 0.06, respectively. There are no correlation between E_{NH} ratios and the corresponding random contacts.

Although the random contacts with values lower than 0.9 % are considered insignificant, we have computed the enrichment ratio of C···C, N···O and O···C short contacts for compounds **1-4**. It is interesting to observe in this type of compounds that the C···C contacts are highly enriched (E_{CC} = 4.86) for compound **2**, enriched for structure **4** (E_{CC} = 1.00), and slightly impoverished for structure **3** (E_{CC} = 0.71), being 0.7 the percentage of R_{CC} for the three compounds. This indicates that E_{CC} and *S*c values show no correlation for structures **2**, **3** and **4**. On the other hand, the high value of E_{CC} for structure **2** helps to explain the exceptional low propensity of the C···H contacts (E_{CH} = 0.73) due to both C···C and C···H contacts are presumably in competition. In the case of structure **3** the high probability to form O···O, C···O and N···O short contacts with enrichment ratios ranging from 1.20 to 2.72, is another reason to explain the reduced value of E_{OH} (0.93), in comparison with the other structures. The X···Y intermolecular contacts which are completely avoided with E_{XY} = 0.00, are not included in Table 5.

4-Conclusions

The molecular structure of 1-(adamantane-1-carbonyl)-3-(2,4,6-trimethylphenyl)thiourea has been determined by single-crystal X-ray diffraction. The dihedral angle between the plane of 2,4,6-tri-methylphenyl fragment and the plane of thiourea moiety is 92.6º for the vacuum isolated molecule, a value very similar to that of 89.56(5)º obtained in the crystal structure determination. All the cyclohexane rings in the adamantane group adopt a very slightly distorted chair conformation as reflected by q(3) value of 0.625Å. The Hirshfeld surfaces, fingerprint plots and

enrichment ratios were found to be very useful in the study of the intermolecular interactions, and their quantitative contributions towards the crystal packing of a series of six 1-(adamantane-1-carbonyl)-3-substituted-phenyl thioureas. The results revealed remarkable relative contributions in H···H interactions more than other contacts. There are structural similarities for the compounds **1, 5** and **6**, such as the presence of N–H···O and C–H···S hydrogen bonds forming centrosymmetric $R_2^2(12)$ and $R_2^2(14)$ dimers, respectively, related with the nature of substituents on the tri-substituted-phenyl ring. According to the enrichment ratios the H···H contacts are favoured, and the S···H contacts have high propensity to form in crystals for all the structures. The O···H and C···H contacts displayed high propensity to occur in five structures. The presence of the less common C–H···F and C–H···Cl hydrogen bonds, as well as π···π and C–H···π contacts, showed be as important as the conventional interactions to direct the packing of molecules. These results could be applied in crystal engineering for the design of supramolecular arrangements using the 1-(adamantane-1-carbonyl)-thiourea synton.

5-Acknowledgments

MFE is a member of the Carrera del Investigador of CONICET (República Argentina). The Argentinean author thanks to the Consejo Nacional de Investigaciones Científicas y Técnicas (CONICET), the ANPCYT and to the Facultad de Ciencias Exactas, Universidad Nacional de La Plata for financial support.

6-References

1. E. Neucki, *Ber. Dtsch. Chem. Ges.*, 1873, **6**, 598-600.
2. G. A. Hope, R. Woods, S. E. Boyd and K. Watling, *Colloids Surf. A*, 2004, **232**, 129-137.
3. L. Guang-yi, Z. Hong, X. Liu-yin, W. Shuai and X. Zheng-he, *Miner. Eng.*, 2011, **24**, 817-824.

4. E. Otazo-Sanchez, L. Pérez-Marin, O. Estevez-Hernandez, S. Rojas-Lima and J. Alonso-Chamarro, *J. Chem. Soc., Perkin Trans. 2*, 2001, 2211-2218.

5. D. Wilson, M. Á. Arada, S. Alegret and M. del Valle, *J. Hazard. Mater.*, 2010, **181**, 140-146.

6. A. I. Daud, W. M. Khairul, H. Mohamed Zuki and K. KuBulat, *J. Sulfur Chem.*, 2014, **35**, 691-699.

7. M. Afzaal, M. A. Malik and P. O'Brien, *J. Mat. Chem.*, 2010, **20**, 4031-4040.

8. J. C. Bruce, N. Revaprasadu and K. R. Koch, *New J. Chem.*, 2007, **31**, 1647-1653.

9. A. Saeed, U. Flörke and M. F. Erben, *J. Sulfur Chem.*, 2014, **35**, 318-355.

10. A. Solinas, H. Faure, H. Roudaut, E. Traiffort, A. Schoenfelder, A. Mann, F. Manetti, M. Taddei and M. Ruat, *J. Med. Chem.*, 2012, **55**, 1559-1571.

11. C. Li, W. Yang, H. Liu, M. Li, W. Zhou and J. Xie, *Molecules*, 2013, **18**, 15737-15749.

12. G. Hallur, A. Jimeno, S. Dalrymple, T. Zhu, M. K. Jung, M. Hidalgo, J. T. Isaacs, S. Sukumar, E. Hamel and S. R. Khan, *J. Med. Chem.*, 2006, **49**, 2357-2360.

13. M. Boiocchi, L. Del Boca, D. E. Gomez, L. Fabbrizzi, M. Licchelli and E. Monzani, *J. Am. Chem. Soc.*, 2004, **126**, 16507-16514.

14. M. Bonizzoni, L. Fabbrizzi, A. Taglietti and F. Tiengo, *Eur. J. Org. Chem.*, 2006, **2006**, 3567-3574.

15. H.-L. Chen, Z.-F. Guo and Z.-l. Lu, *Org. Lett.*, 2012, **14**, 5070-5073.

16. S. Li, X. Cao, C. Chen and S. Ke, *Spectrochim. Acta*, 2012, **96A**, 18-23.

17. C. Limban, A.-V. Missir, I. C. Chirita, A. F. Neagu, C. Draghici and M. C. Chifiriuc, *Rev. Chim. (Bucharest)*, 2011, **62**, 168-173.

18. C. Limban, A.-V. Missir, I. C. Chirita, C. D. Badiceanu, C. Draghici, M. C. Balostescu and O. Stamatoiu, *Rev. Roum. Chim.*, 2008, **53**, 595-602.

19. J. Müller, C. Limban, B. Stadelmann, A. V. Missir, I. C. Chirita, M. C. Chifiriuc, G. M. Nitulescu and A. Hemphill, *Parasitol. Int.*, 2009, **58**, 128-135.

20. J. Sun, S. Cai, H. Mei, J. Li, N. Yan, Q. Wang, Z. Lin and D. Huo, *Chem. Biol. Drug Des.*, 2010, **76**, 245-254.

21. F. F. Ferreira, A. C. Trindade, S. G. Antonio and C. de Oliveira Paiva-Santos, *CrystEngComm*, 2011, **13**, 5474-5479.

22. R. Custelcean, N. L. Engle and P. V. Bonnesen, *CrystEngComm*, 2007, **9**, 452-455.

23. J. Huang, R. L. Ostrander, A. L. Rheingold and M. A. Walters, *Inorg. Chem.*, 1995, **34**, 1090-1093.

24. K. S. Eccles, R. E. Morrison, A. R. Maguire and S. E. Lawrence, *Cryst. Growth Des.*, 2014, **14**, 2753-2762.

25. K. S. Eccles, R. E. Morrison, A. S. Sinha, A. R. Maguire and S. E. Lawrence, *Cryst. Growth Des.*, 2015, **15**, 3442-3451.

26. D. Dey, T. P. Mohan, B. Vishalakshi and D. Chopra, *Cryst. Growth Des.*, 2014, **14**, 5881-5896.

27. I. Wawrzycka-Gorczyca, *J. Struct. Chem.*, 2014, **55**, 520-524.

28. S. B. Novaković, B. Fraisse, G. A. Bogdanović and A. Spasojević-de Biré, *Cryst. Growth Des.*, 2007, **7**, 191-195.

29. B. M. Yamin and U. M. Osman, *Acta Crystallogr.*, 2011, **E67**, o1286.

30. W. Zhu, W. Yang, W. Zhou, H. Liu, S. Wei and J. Fan, *J. Mol. Struct.*, 2011, **1004**, 74-81.

31. O. Estévez-Hernández, J. Duque, J. Ellena and R. S. Correa, *Acta Crystallogr.*, 2008, **E64**, o1157.

32. A. Okuniewski, J. Chojnacki and B. Becker, *Acta Crystallogr.*, 2012, **E68**, o619-o620.

33. X. Zhang, H. He, M. Xu and P. Zhong, *J. Chem. Res.*, 2011, **35**, 323-325.

34. N. Gunasekaran, R. Karvembu, S. W. Ng and E. R. T. Tiekink, *Acta Crystallogr. E*, 2010, **66**, o2113.

35. H. Pérez, R. S. Correa, A. M. Plutin, B. O'Reilly and M. B. Andrade, *Acta Crystallogr. C*, 2012, **68**, o19-o22.

36. L. R. Gomes, L. M. N. B. F. Santos, J. A. P. Coutinho, B. Schroder and J. N. Low, *Acta Crystallogr. E*, 2010, **66**, o870.

37. A. Saeed and U. Flörke, *Acta Crystallogr. E*, 2006, **62**, o2403-o2405.

38. G. Binzet, F. M. Emen, U. Flörke, T. Yesilkaynak, N. Külcü and H. Arslan, *Acta Crystallogr. E*, 2009, **65**, o81-o82.

39. M. K. Rauf, A. Badshah and U. Flörke, *Acta Crystallogr. E*, 2006, **62**, o3823-o3825.

40. A. Saeed, A. Khurshid, M. Bolte, A. C. Fantoni and M. F. Erben, *Spectrochim. Acta*, 2015, **143A**, 59-66.

41. A. Saeed, M. F. Erben and M. Bolte, *Spectrochim. Acta*, 2013, **102A**, 408-413.

42. A. Saeed, U. Flörke and M. F. Erben, *J. Mol. Struct.*, 2014, **1065-1066**, 150-159.

43. C. Janiak, *J. Chem. Soc., Dalton Trans.*, 2000, 3885-3896.

44. S. K. Seth, D. Sarkar and T. Kar, *CrystEngComm*, 2011, **13**, 4528-4535.

45. S. K. Seth, P. Manna, N. J. Singh, M. Mitra, A. D. Jana, A. Das, S. R. Choudhury, T. Kar, S. Mukhopadhyay and K. S. Kim, *CrystEngComm*, 2013, **15**, 1285-1288.

46. P. Manna, S. K. Seth, M. Mitra, A. Das, N. J. Singh, S. R. Choudhury, T. Kar and S. Mukhopadhyay, *CrystEngComm*, 2013, **15**, 7879-7886.

47. S. K. Seth, I. Saha, C. Estarellas, A. Frontera, T. Kar and S. Mukhopadhyay, *Cryst. Growth Des.*, 2011, **11**, 3250-3265.

48. S. K. Seth, D. Sarkar, A. D. Jana and T. Kar, *Cryst. Growth Des.*, 2011, **11**, 4837-4849.

49. S. K. Seth, *CrystEngComm*, 2013, **15**, 1772-1781.

50. P. Hohenberg and W. Kohn, *Phys. Rev.*, 1964, **136**, B864-B871.

51. W. Kohn and L. Sham, *Phys. Rev.*, 1965, **140**, A1133-A1138.

52. A. Becke, *Phys. Rev. A*, 1988, **38**, 3098-3100.

53. C. Lee, W. Yang and R. G. Parr, *Phys. Rev. B*, 1988, **37**, 785-789.

54. Gaussian 03, Revision C.02, M. J. Frisch, G. W. Trucks, H. B. Schlegel, G. E. Scuseria, M. A. Robb, J. R. Cheeseman, J. A. Montgomery Jr., T. Vreven, K. N. Kudin, J. C. Burant, J.

M. Millam, S. S. Iyengar, J. Tomasi, V. Barone, B. Mennucci, M. Cossi, G. Scalmani, N. Rega, G. A. Petersson, H. Nakatsuji, M. Hada, M. Ehara, K. Toyota, R. Fukuda, J. Hasegawa, M. Ishida, T. Nakajima, Y. Honda, O. Kitao, H. Nakai, M. Klene, X. Li, J. E. Knox, H. P. Hratchian, J. B. Cross, C. Adamo, J. Jaramillo, R. Gomperts, R. E. Stratmann, O. Yazyev, A. J. Austin, R. Cammi, C. Pomelli, J. W. Ochterski, P. Y. Ayala, K. Morokuma, G. A. Voth, P. Salvador, J. J. Dannenberg, V. G. Zakrzewski, S. Dapprich, A. D. Daniels, M. C. Strain, O. Farkas, D. K. Malick, A. D. Rabuck, K. Raghavachari, J. B. Foresman, J. V. Ortiz, Q. Cui, A. G. Baboul, S. Clifford, J. Cioslowski, B. B. Stefanov, G. Liu, A. Liashenko, P. Piskorz, I. Komaromi, R. L. Martin, D. J. Fox, T. Keith, M. A. Al-Laham, C. Y. Peng, A. Nanayakkara, M. Challacombe, P. M. W. Gill, B. Johnson, W. Chen, M. W. Wong, C. Gonzalez and J. A. Pople, Gaussian, Inc., Wallingford CT, 2004.

55. M. J. Frisch, J. A. Pople and J. S. Binkley, *J. Chem. Phys.*, 1984, **80**, 3265-3269.

56. G. Sheldrick, *Acta Crystallogr.*, 2008, **A64**, 112-122.

57. L. Farrugia, *J. Appl. Crystallogr.*, 1999, **32**, 837-838.

58. M. Nardelli, *Comput. Chem.*, 1983, **7**, 95-98.

59. M. Nardelli, *J. Appl. Crystallogr.*, 1995, **28**, 659.

60. J. L. Farrugia, *J. Appl. Crystallogr.*, 1997, **30**, 565.

61. C. F. Macrae, I. J. Bruno, J. A. Chisholm, P. R. Edgington, P. McCabe, E. Pidcock, L. Rodriguez-Monge, R. Taylor, J. van de Streek and P. A. Wood, *J. Appl. Crystallogr.*, 2008, **41**, 466-470.

62. J. J. McKinnon, D. Jayatilaka and M. A. Spackman, *Chem. Comm.*, 2007, 3814-3816.

63. M. A. Spackman and D. Jayatilaka, *CrystEngComm*, 2009, **11**, 19-32.

64. M. A. Spackman, *Phys. Scr.*, 2013, **87**, 048103.

65. J. J. McKinnon, M. A. Spackman and A. S. Mitchell, *Acta Crystallogr.*, 2004, **60B**, 627-668.

66. S. K. Wolff, D. J. Grimwood, J. J. McKinnon, M. J. Turner, D. Jayatilaka and M. A. Spackman, CrystalExplorer (Version 3.1) University of Western Australia, 2012.

67. S. K. Seth, D. Sarkar, A. Roy and T. Kar, *CrystEngComm*, 2011, **13**, 6728-6741.

68. S. K. Seth, *Inorg. Chem. Comm.*, 2014, **43**, 60-63.

69. P. Manna, S. K. Seth, A. Das, J. Hemming, R. Prendergast, M. Helliwell, S. R. Choudhury, A. Frontera and S. Mukhopadhyay, *Inorg. Chem.*, 2012, **51**, 3557-3571.

70. H. M. Abosadiya, E. H. Anouar, S. A. Hasbullah and B. M. Yamin, *Spectrochim. Acta*, 2015, **144A**, 115-124.

71. D. M. Gil, M. E. Defonsi Lestard, O. Estévez-Hernández, J. Duque and E. Reguera, *Spectrochim. Acta*, 2015, **145A**, 553-562.

72. M. Atiş, F. Karipcin, B. Sarıboğa, M. Taş and H. Çelik, *Spectrochim. Acta*, 2012, **98A**, 290-301.

73. M. S. M. Yusof, R. H. Jusoh, W. M. Khairul and B. M. Yamin, *J. Mol. Struct.*, 2010, **975**, 280-284.

74. A. Saeed, M. F. Erben and U. Flörke, *J. Mol. Struct.*, 2010, **982**, 91-99.

75. O. Estévez-Hernández, E. Otazo-Sánchez, J. L. Hidalgo-Hidalgo de Cisneros, I. Naranjo-Rodríguez and E. Reguera, *Spectrochim. Acta*, 2005, **A62**, 964-971.

76. L. Bistricic, G. Baranovic and K. Mlinaric-Majerski, *Spectrochim. Acta*, 1995, **51A**, 1643-1664.

77. W. Yang, W. Zhou and Z. Zhang, *J. Mol. Struct.*, 2007, **828**, 46-53.

78. P. P. Tadbuppa and E. R. T. Tiekink, *Acta Cryst.*, 2007, **E63**, o1779-o1780.

79. A. Saeed, A. Khurshid, J. P. Jasinski, C. G. Pozzi, A. C. Fantoni and M. F. Erben, *Chem. Phys.*, 2014, **431-432**, 39-46.

80. Z. Weiqun, L. Baolong, Z. liming, D. Jiangang, Z. Yong, L. Lude and Y. Xujie, *J. Mol. Struct.*, 2004, **690**, 145-150.

81. M. K. Rauf, A. Badshah and M. Bolte, *Acta Crystallogr. E*, 2006, **62**, o2444-o2445.

82. D. Cremer and J. A. Pople, *J. Am. Chem. Soc.*, 1975, **97**, 1354-1358.

83. S. K. Mohamed, A.-A. M. Jaber, S. Saeed, K. S. Ahmad and W.-T. Wong, *Acta Crystallogr. E*, 2012, **68**, o1597.

84. R. Kumar, M. Elango, R. Parthasarathi, D. Vijay and V. Subramanian, *J. Chem. Sci.*, 2012, **124**, 193-202.

85. A. Spek, *Acta Crystallogr.*, 2009, **D65**, 148-155.

86. C. Jelsch, K. Ejsmont and L. Huder, *IUCrJ*, 2014, **1**, 119-128.

87. G. R. Desiraju and T. Steiner, *The Weak Hydrogen Bond in Structural Chemistry and Biology*, Oxford University Press, Oxford, 1999.

88. C. Jelsch, S. Soudani and C. Ben Nasr, *IUCrJ*, 2015, **2**, 327-340.

The 1-acyl thiourea synton is characterized through a complete Hirshfeld surfaces analysis for a series of six closely related 1-(adamantane-1-carbonyl) thioureas.